Pollution induced mass-deformities in *Tripneustes*: Biomechanical aspects

J. Dafni
Ben-Gurion University, Eilat Campus, Box 6469 Eilat, Israel

ABSTRACT: In the late 1970's two cases of skeletal mass-deformities were discovered in *Tripneustes gratilla elatensis* populations in polluted areas, at Eilat, Israel: One, characterized by tall, highly distorted tests and the second, apical depressed flatter urchins. In the 1980's the deformities disappeared, to re-appear in 2005. Extensive research was carried out to identify the pollutants, industrial calcification inhibitors, and elucidate the mechanism involved. Evidence is provided here for the hypothesis that 4 factors were involved in this process: calcification inhibition, sutural collagen 'softening', and mechanical activity of contractile and elastic components and finally, 'post-traumatic' calcification, including resorption and allocation of $CaCO_3$ in the interior body wall to stabilize the deformed tests. Of several sea urchin species present in the area, only *Tripneustes* showed such deformities, which may be related to the fragility of the test. Results support the biomechanical model of growth and morphogenesis of the echinoid tests.

1 INTRODUCTION

1.1 *Mass-deformities in Tripneustes*

Post-larval deformities in regular echinoids are uncommon, mainly attributed to abnormal regeneration from a traumatic injury by predators or parasites (Moore, 1974; Allain, 1978). Mass-deformities are extremely rare. The first historic record was entered in the late 1800's by l'Oriol, (1883, cited by Mortensen, 1943), who wrote that mass deformities prevailed for sometime in a *Tripneustes gratilla* population in Mauritius Island. Our present reports seem to be unique in modern time.

Throughout the late 1970's, two mass deformities were discovered in the sea urchin *Tripneustes gratilla elatensis* (Dafni, 1983a) in polluted sites at Eilat, northern Red Sea. The deformities were of two different types: Type A showing excessive bulging of the upper half, with height to diameter ratio (H/D) reaching 1.4 (Fig. 1a) were found near a waste water runoff from a power station combined with a desalination plant, emitting hot (39^0C) and saline ($45\ ^0/_{00}$.) water (Site A, Dafni, 1980). Type B was flatter (H/D < 0.4), with deep aboral depressions (Fig. 1b). It was shown by > 65% of a small *T. g. elatensis* population in an artificial lagoon (Site B), next to a runoff pipe, ejecting laundry wastewater from a neighboring hotel (Dafni, 1983b). In a subsequent study (Dafni & Erez, 1987b) various aspects of the deformities were examined, and thoroughly analyzed. Chemical pollution is the most plausible cause to these deformities.

The deformities disappeared in early 1980's, when the power plant closed. Ecological conditions in the artificial lagoon deteriorated, and all echinoid species disappeared. In the 2005, however, type B deformity reappeared in a 200 m stretch of shore line between a new hotel and a submarine restaurant, 50 m offshore (Site C). Most characteristics shown there are similar to type B deformity, as described (Dafni, 1983b).

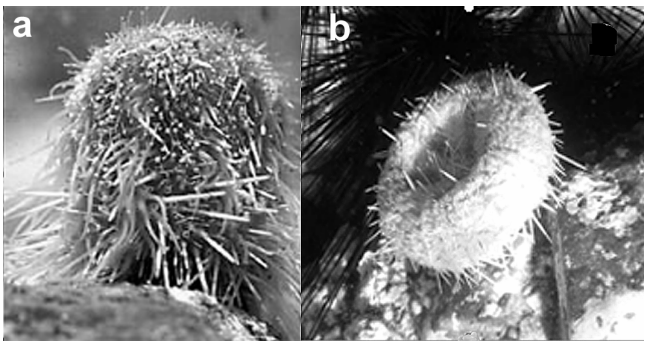

1. Two types of skeletal deformities in *Tripneustes gratilla elatensis.* a. Exaggerated vertical growth and bulging upper half (type A). b. Same subspecies, exhibiting flatter tests, with deep aboral depressions (type B).

1.2 *Working hypothesis*

Although these phenomena were well documented and studied (Dafni, 1980, 1983b, Dafni & Erez, 1987b), no conclusion was reached concerning the underlying mechanism for test distortion. This paper aims to examine post-deformity growth and deformation processes in light of a biomechanical model presented by the author (Dafni, 1986), and subsequent modifications (Ellers, 1993, Ellers et al., 1998; Johnson et al. 2002), adding new evidence and insight.

A working hypothesis that explains the deformities is the result of four processes:

1 Calcification inhibition that reduces the test growth and impairs its rigidity.

2 The pollutant/s affect the mechanical properties of the collagenous sutural fibers, thus enabling uncontrolled growth of individual plates.

3 Biomechanical effects caused by contractile and elastic elements – mainly intestine mesenterial filaments, that distort test morphology.

4. "Post-traumatic" abnormal calcification that stabilizes and fixes the deformed shape.

2 MATERIALS AND METHODS

2.1 *Possible pollutants*

Five reagents, industrial $CaCO_3$ and $CaPO_4$ deposition inhibitors, effective under high temperatures, were used at different times to maintain the pipe system of the power plant (ingredients supplied by the producers). We tested these reagents in our experiments, as potential pollutants, responsible to type A deformity:

- Monsanto Dequest 2060. Diethylenetriamine-penta (methylene phosphonic acid).
- Monsanto Dequest 2054. Potassium salt of hexamethylenediamine-tetra (methylene phosphonic acid).
- P-70 (Cyanamid). Sodium polyacrylate.
- Belgard EV (Ciba-Geigy). Based on polymeric carboxylic acid.
- CYAF 5021 (Cyanamid). Acrylamide-sodium acrylate resin.
- The pollutant that was suspected to cause type B deformity was a detergent, N-200 (Zohar, Israel), applied in the hotel's laundry to reduce $CaCO_3$ pipe clogging. It also contained phosphates, sulfonate and non-ionic detergents.

To examine hypothesis that collagen synthesis and alignment inhibitors were among the pollutants, the following reagents, known to affect collagen synthesis (Harkness, 1968), were applied by injection of 20-50 mg through the peristome membrane 7-14 days before radioactive exposure (Dafni & Erez, 1987b):

- β–mercaptoethyleneamine (MEA), known as Lathyrogen
- β–aminoproprionitrile (APN), known as Antielastin

Both are products of Sigma Co. USA

2.2 *Growth experiments*

In experiment 1, 22 of type A deformed *T. g. elatensis*, collected in site A, were maintained individually or in small groups in through-flowing seawater tanks for up to 2 years. The urchins were fed *ad libitum* their natural food, turf algae mixed with *Ulva lactuca* leaves. Horizontal and vertical sizes were recorded initially and at the end of the experiment. All measurements were taken with plastic calipers with the precision of 0.1 mm, and the average of 5 measurements recorded. For each individual the diameter size was determined, and the ratio between vertical and horizontal sizes (H/D ratio) calculated.

2.3 *Radiotracer experiments*

Morphometric studies of both deformities (Dafni, 1980, 1983b) showed excessive growth in the vertical dimension but the number of plates per longitudinal column was not different from normal conspecifics. In deformed individuals each plate grew excessively in the vertical dimension.

An experiment, using $^{45}CaCO_3$ was conducted to assess the influence of pollutants on the differential calcification process (for methodology, see Dafni & Erez, 1987a).

In experiment 3 (Dafni & Erez, 1987a) the tested reagents were added 7 days prior to exposure of sea urchins to ^{45}Ca seawater, for 8 hours, at a concentration of 0.02% (v/v), 1-5% of the lethal dose, according to producers' declaration.

In these experiments the incorporation of Ca, was measured for whole tests and for individual interambulacral (IA) plates (Dafni & Erez, (1987a). Since each test plate grows at a different rate in its various directions (Märkel, 1975; Dafni & Erez, 1987a), we developed an arbitrary measure, v/h ratio, to quantify the sutural calcification in the vertical direction (adapical and adoral) of IA plates vs. calcification in the horizontal direction (interradial and adradial sutural margins), using the following procedure:

From the sampled plate ca. 0.5 mm was scraped-off from the plate edge, in all 4 margins, and the radioactive Ca uptake per unit weight for each margin measured, and calculated using the equation

$$\text{v/h ratio}=(\text{adap}+\text{ador})/(\text{interrad}+\text{adrad}) \quad (1)$$

where

adap=adapical, ador=adoral margins

interred=interradial and adrad=adradial margins

2.4 *Microscopic and macroscopic observations of deformed T. g. elatensis*

Light microscopy and SEM images were made during the original study (Dafni, 1980, 1983b, 1986). Some of these observations are reviewed here in light of new information and further interpretation. For technical details see Dafni (1986).

3 RESULTS

3.1 *Long-range growth patterns of deformed T. g. elatensis*

The results of Experiment 1, of Type A deformed urchins growth patterns (Fig. 2) exhibit two contradicting trends:

1. The H/D ratio of a normal *T. g. elatensis* is ca 0.55 (Fig. 3). All deformed individuals taking part in this growth experiment had initially abnormal H/D ratio (> 0.6). The larger the urchin was initially; the less deformed is was (lower H/D).
2. During the experiment, most of the smaller urchins, already deformed, did not increase their horizontal size, but continued to deform (increased their H/D ratio). Only several, less deformed smaller individuals grew without further deforming. Urchins larger than 60 mm animals showed no horizontal growth for over a year, and a very slight change in their H/D ratio.

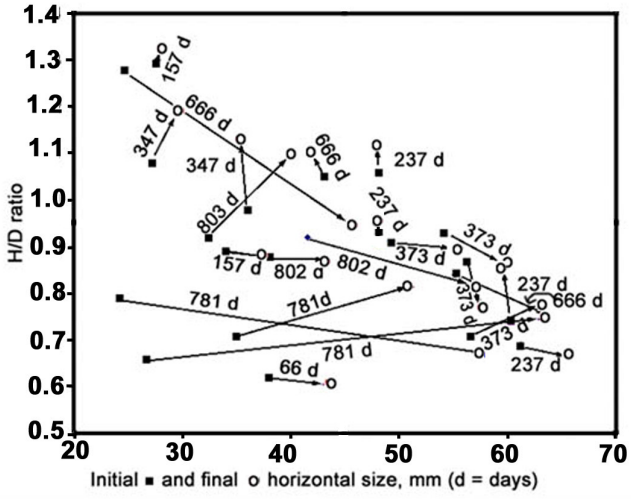

Figure 2. Change in size and H/D ratio during maintenance in captivity of type A deformed urchins. Arrows connects initial (squares) with final (hollow circles) size and H/D of the same individuals. Next to the growth arrows, time elapsed between initial and final measurements.

On the other hand, all deformity type B urchins were larger than 50 mm, when collected. Their diameter did not increase for > 2 years, and their tests showed a compact stereom (low porosity).

3.2 *Effect of pollutants on non-deformed T. g. elatensis*

In experiment no. 2, five groups of 5-11 individuals each of small (ca. 20 mm) non-deformed *T. g. elatensis* were exposed for 70 days to the reagents, used at different times in the adjacent power plant. In all groups horizontal diameter growth was arrested, while control group assumed normal growth. All, except one (Monsanto Dequest 2060, not included in the graph) showed significant decrease of H/D ratio (Fig.3). In one case (urchins exposed to CYAF 5021) the experiment was terminated after 45 days, when most of the urchins' tests disintegrated (* in Fig. 3).

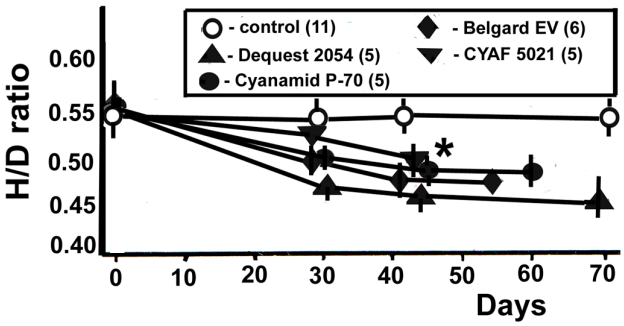

Figure 3. Vertical to horizontal (H/D) ratio +/- SD change in a long-term exposure of non-deformed urchins to 4 industrial calcification reagents. In parentheses=number of tested urchins.

3.3 *Sutural collagen inhibition*

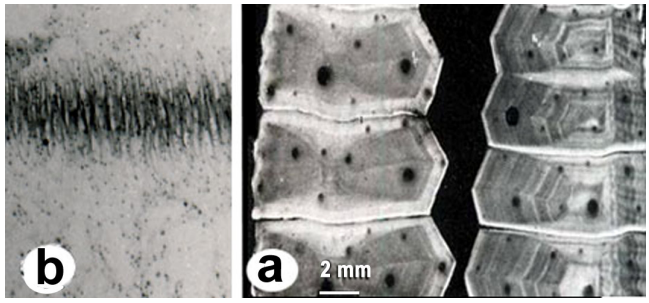

Figure 4a. Comparison of a normal (right) and deformed urchins' IA plate column, charred and xylene immersed (Dafni, 1980). The left column shows abnormal growth patterns, of plates growing almost equally in all directions, a pattern quantified by the v/h ratio; b. Collagen fibers striding across the latitudinal suture of an active growing IA plate column.

Figure 4a shows a normal and typical IA plate column of type A deformed urchin, at ambitus level. The excessive H/D ratio in these urchins has been evidently achieved by abnormal accretion of the latitudinal sutures (longitudinal direction). Our observations have shown that rapidly growing sutures are characterized by long and conspicuous fibers (Dafni, 1986). Finding developed collagen fibers at the lati-

tudinal suture (Fig. 4b) suggests that the pollutant(s) affected the collagen fibers tightness along these sutures, encouraging excessive growth. In non-deformed urchins this suture shows fewer fibers.

3.4 *Pollutants influence on differential growth*

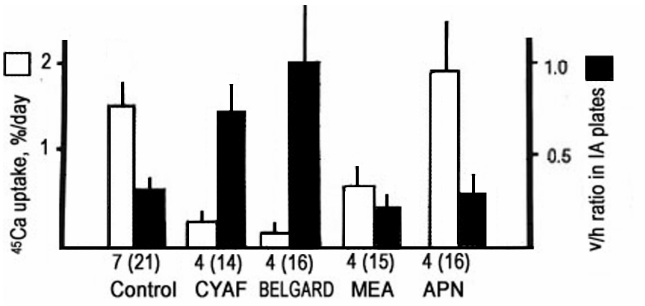

Figure 5. Calcification rates, means +/- SD (^{45}Ca uptake in %/day) of whole ambital plates of *T. g. elatensis* exposed to different pollutants (white columns), and v/h ratio of the ambital plates (dark columns). Below: number of tested sea urchins and number of analyzed plates (in parentheses).

Experiment no. 3 tested the effect of 4 possible pollutants on the differential growth of individual IA ambital plates of non-deformed *T. g. elatensis*. The results are shown in Figure 5: Per plate ^{45}Ca uptake (white columns) was low in all treatments, except APN, compared to the control. Change in differential calcification of individual plates (increase in v/h ratio) was significant for CYAF and Belgard. Collagen synthesis inhibitors, APN and MEA, did not provide significant results.

The significant increase in the v/h ratio of individual plates in sea urchins treated with Belgard and CYAF may be used as a predictor of abnormal growth of *T. g. elatensis* upon exposure to these pollutants.

There is no clear evidence which of the above reagents caused the deformities, but this experiment shows that both CYAF and Belgard, and possibly other reagents in this list could do it.

3.5 *Mechanical activity of tensile and contractile elements*

The third factor in our hypothesis is distortion of the coronal test of the deformed urchins. Older work on anatomy (Dafni, 1983b, Dafni & Erez, 1987b) showed that echinoid intestine (gut) follows a distinct pattern within the test. Upon emergence from the lantern, it makes two whorls in the coelom cavity: The foregut turns clockwise for a whole round, U- turns counterclockwise to proceed as hindgut, before climbing to the anus. Mesenterial filaments connect it to the body wall across the ambulacra (Amb), whereas the hindgut "covers" the foregut.
The observation that these filaments, made mainly from collagen, are imbedded with muscle fibers (Dafni, 1983b) predicts that they may be involved in mechanical tethering activity. And indeed, there are two uppermost attachment points of the mesenterial system. We found that these critical points in the deformed urchins' morphology are related to the deformities:

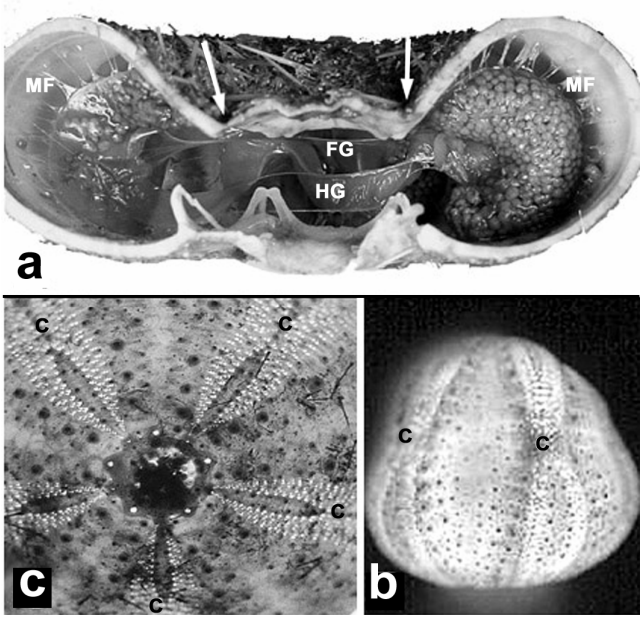

Figure 6a. Aborally depressed type B deformed 60 mm *T. g. elatensis*, showing the two whorls of the gut, foregut (FG) and hindgut (HG), whose mesenterial filaments (MF) connected to IA plates of the body wall. Arrows point at deep pits that coincide with the uppermost attachment of the hindgut mesenterial filaments. b. Type A deformed 45 mm urchin's test, lateral view (illuminated from within), showing the Amb constrictions (c), coinciding with the uppermost attachment points of the foregut, at approx. 2/3 of their height. c. Another type A deformed test, apical view, displaying a symmetrical array of pinches (c), constrictions of the Amb columns, appearing in many type A deformed urchins.

1. The hindgut upper attachment point is anchored next to the apex. If our hypothesis is correct, pulling down at this critical point, under conditions of a less rigid test, causes deformity B. In some extreme cases, the entire apical dome collapses, resting on top of the lantern (Fig. 6a).
2 . The second attachment point, of the foregut, is at 2/3 of the test height. Here the mesenterial filaments stride over the Amb columns. This critical point is the lowest end of the apical distorted bulges, typical of many type A deformed *T. g. elatensis*.
3. The latter attachment point, in most of type A deformities, exhibits Amb constrictions (="pinches") (Fig. 6B, C).

I propose that both deformities are initiated by reduction of the close-fit of ill-calcified plates, and a "softened" sutural collagen fiber system. Under these conditions, the coronal test yields to tethering of the mesenterial filaments, that either cause aboral

collapse, or excessive vertical growth, typical to deformity A.

3.6 *"post- traumatic" calcification*

Figure 7 shows type B deformed urchins, indicating "remodeling" of their inner plates' surface, apparently occurring after reaching their final deformed shape. It included resorption (R) of the spongy layer (SL), and skeletal deposition in other sites. Noteworthy are thickening of the IA plates suture (S), and creation of protuberances (MB) at the mesenterial fibers bases. Deformed urchins' plates show a distinct compact layer (CL), which explains the lower porosity shown by most deformed *T. g. elatensis* urchins.

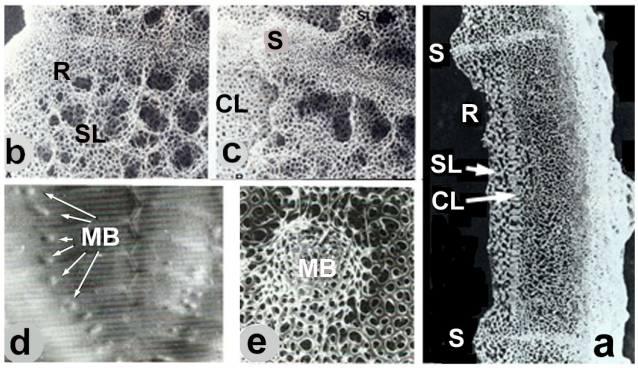

Figure 7. Remodeling of deformed type B *T. g. elatensis*: a. SEM picture of IA plate longitudinal section; b. Eroded inner spongy layer (SL); c. Thickened sutures (S), above an inner eroded spongy layer, exposing the stereom compact layer (CL). d. Mesenterial bases protuberances, enhanced by post-deformation calcification (natural size). e. SEM picture of one such protuberance (size ~1mm).

4 DISCUSSION

4.1 *Role of mechanical factors in urchin morphology*

A regular sea urchin test is rigid peripherally and hollow, filled with fluid and soft tissue internally. Thompson (1917) wrote that "the rigidity of the shell is more apparent than real". And indeed, the deformities reported here exhibit the apparent rigidity, that consists of two main elements: rigid, close-fitted calcareous plates, and flexible, tension resistant collagenous fibers, that attach to the plates across the sutures. The distribution of the sutural collagenous fibers is of great importance. They are longer, denser and well aligned in fast growing sutures, and short, sparse, and much less organized in sutures that grow slowly or do not grow at all. Generally, the longitudinal sutures of both Amb and IA, are faster growing, showing accordingly long and developed collagenous fiber bands. The latitudinal sutures are usually slow growing to accommodate for newly formed plates that appear in uppermost end of each column. So, both IA and Amb plates are narrow in the vertical dimension, which reflects in their differential growth pattern (low v/h ratio).

Our observations showed that normally the adoral, lower half of the test consists of smaller plates, showing negligible accretion, and maximal rigidity, and stiff sutural cohesion. The upper, adapical half, is the faster growing, characterized by a wide band of long collagenous fibers, at least in the horizontal direction. Dafni (1986) suggested that these fibers play two roles in the urchin's morphogenesis: (1) they prevent excessive growth in compressed sutures and (2), encourage rapid growths in sutures where tensional stresses prevail, by directing the stereom trabeculae to penetrate between them. Johnson et al. (2002) discussed that the collagenous fibers that possess the ability to become stiff or soft, under neural control (Wilkie, 1996) are actually the main morphogenetic agent that controls the echinoid skeletal patterns.

In mechanical terms, the upper half of the test is a dome-like structure. Immaterial whether there is a significant internal pressure supporting the test from within (Dafni, 1986; Ellers et al., 1998), or it is negligible (Ellers & Telford, 1992), two main factors may distort, or even collapse the echinoid "dome": faulty calcification, that reduces the plates close-fitting, and collagen stiffness, that ensures its flexibility. In experiment 2, normal, fast-growing *T. g. elatensis* juveniles, stopped to grow and calcify, and their collagen fibers also softened when exposed to the pollutants. Their entire test became pliable, and flatter (Fig. 3). Ultimately, one group showed total test disintegration (Asterisk in Fig. 3).

The role of the sutural fibers in this context is less clear. They are part of a connective tissue envelope in which the test plates grow (Moss & Meehan, 1967), and a positive relation exists between their loosening and sutural accretion (Johnson et al., 2002). We found that the relative thickness of the sutural fiber band correlates with the growth rate and calcification of the particular suture (Dafni, 1986; Dafni & Erez, 1987a), suggesting that stiff, less pliant arrangement of these fibers across a suture, inhibits growth and calcification of the sutural margins.

The observation that deformed *T. g. elatensis* IA plates of both types show excessive growth in the direction, reflected in high v/h ratio (Figs. 4a, 5) when exposed to the pollutants, is possible evidence that the collagenous fibers underwent abnormal loosening in the latitudinal sutures. Unfortunately, the v/h ratio of urchins' plates, treated by APN and MEA, collagen inhibitors, did not provide conclusive evidence. An alternative suggestion is that calcium-dependent cellular processes, involved in the stiffening response of echinoderms (Trotter & Koob, 1995), is related to Ca deficiency produced by the afore-mentioned calcification inhibitors.

The involvement of a third factor – mesenterial filaments - is strongly supported by the observation that deformity B was not a passive collapse of the "apical dome", as it was pulled down at precise points around the border between the apex and the uppermost IA plates, creating conspicuous deeper pits (Fig. 6a). The most likely factor to create type B deformities is the mesenterial filaments that attach the hindgut to the body wall (Fig. 6a). In deformity A the involvement of the foregut mesentery filaments is well established by the appearance of Amb constrictions (Fig. 6b , c), and by the fact that the urchins shown a distorted shape, with critical points coincident with the attachment points of the hindgut, at 2/3 of its height. .

4.2 *The deformities and the biomechanical models*

Several models were presented to define the constructional elements whose presence or activities maintain or modify the echinoid test. In a biomechanical model for the morphogenesis (Dafni, 1986), several structural elements that influence the test plates' differential growth were presented:

1. The inner pressure of the internal fluids and organs growth exert pressure, analogous to the inner pressure in liquid drops.

2. Analogous to the surface tension of a drop, are the close-fitted calcareous plates, tied together along sutures by collagenous fibers (=ligaments), that provide its flexibility.

Yet interplay between several structural elements modifies the growth patterns, and accounts for its growth and morphology variations:

2a. Tube-feet exert forces that pull the Amb column at the substrate. Dafni, (1986) showed that *T. g. elatensis* that moved to a soft-bottom habitat and had reduced pull, changed the H/D ratio accordingly, as well as their differential calcification (Dafni & Erez, 1987b, Fig. 9b).

2b. Inner tether patterns of the mesenterial filaments (=threads), is responsible to the fine-tuning of the differential growth (Dafni & Erez, 1982).

2c. Regulation of echinoid plates' growth by changes in the mutable sutural collagen (Ellers et al., 1998; Johnson et al., 2002) seems to be rather a passive process that enables the coronal test to close sutural gaps, formed in response to tensional forces, while the main role is played by elements 2a and 2b.

4.3 *Evaluation of our hypothesis*

The above mentioned working hypothesis on the factors that caused the deformities is based on the biomechanical model, and the results should support its validity. ^{45}Ca uptake is by far quicker that any other tagging technique. Using it enabled us to measure growth and morphometric changes in almost real time.

1 Calcification inhibition by the pollutants is confirmed by experiments 2 & 3. Growth and calcification of non-deformed *T. g. elatensis* was lower than non-deformed control (Fig. 5).

2 In deformed urchins, of both types, the plates above the ambitus showed excessive growth in the vertical direction. It showed as growth lines of charred IA plates (Fig. 4a), and in the radioactive assay, as abnormally high v/h ratio (Fig. 5)

The combined effect of both factors decreased rigidity of the upper, faster growing half of the test. Under these conditions, collapse of the "apical dome", as shown in deformity type B (Fig. 6A), is inevitable. This common form of deformity, though less profound, has been found in other studies (Moore, 1974; Allain, 1978; Pawson, in lit.). Less common, and possibly more complex is the deformity type A. Here, the activity of the mesenterial filaments is undeniable. The importance of these filaments is accentuated by the formation of protuberances in the inner surface, where they are attached (Fig. 7d, e).

The results of experiment 1 indicated that type A deformity was not a short-term rapid event, rather an onset of a long-term size dependent process. In smaller (juveniles) *T. g. elatensis* most of the test was distorted. They did not grow in diameter, but continued to deform even after removed from the deleterious environment (left flank in Fig. 2). Larger individuals, on the other hand, showed an upper abnormal half, superimposed on a 'normal' lower half (Fig. 6b). Their change was usually slight (Fig. 2)

Deformity type B apparently was a rapid process that included 'softening' of the aboral half sutures, and a collapse of the apical dome. Once the deformed shape has been obtained, there was no further diameter increase, and the only calcification shown was remodeling of the coronal plates (Fig. 7).

In deformity type A the involvement of mesenterial filaments resulted in no lesser important phenomena, i.e. the Amb constrictions (pinches) that appear mainly in the upper attachment point of the fore gut. It is reasonable to conclude that down pull at these critical points, caused the plates above them to grow in a deformed mode. The symmetric constrictions, shown in Figure 7c, form a 'petaloid', not unlike the irregular echinoids petals (Dafni, 1988), are another demonstration of the apparent mechanical activity of these filaments.

4.4 *Why did only Tripneustes deform?*

A question that haunted me since discovering the first mass-deformed urchins is why *Tripneustes* was the only sea urchin that showed these phenomena. In the polluted areas, *Diadema setosum, Echinothrix calamaris* and *Echinometra mathaei* were common. Occasionally seen there were *Nudechinus scotiopremnus* and *Heterocentrotus mammilatus.* Yet,

none of these sea urchins showed any of the described deformities.

Part of the answer may lie in the extreme fragility of *Tripneustes*. It is by far the fastest growing echinoid species (Ebert, 1975; Dafni, 1992), while having an extremely thin body wall. Ebert (1988) compared allometric parameters for 12 species of regular echinoids, for body components, $C = \alpha T^{\beta}$, where T is total weight. His results show that both populations of *T. gratilla* have the lightest body wall (ca. 30% of total weight, compared with > 47% for Diadematidae, and > 70% in Echinometridae), and the largest coelomic cavity component (ca. 60%, compared with < 45% of the other families), which makes it to be most fragile than any of the analyzed regular echinoids he studied.

Another factor that causes *T. g. elatensis* to be more vulnerable is the smaller number of digitations in the sutures of the individual plates. This has been shown in many SEM pictures. It adds to the relative fragility of *T. g. elatensis* tests, illustrated by its test structure disintegrating soon after they die, while most tests of other regulars remain intact for longer time

These experiments may explain why so few type B deformed *T. g. elatensis* were < 50 mm HD. I believe that smaller sea urchins exposed to the pollutants either totally collapsed or taken immediately by predators. Larger type B deformed had more survival chance, due to their many pedicellaria and thicker body wall. This is well indicated in measurements: Most of the deformed urchins' tests were more compact than normal *T. g. elatensis* (Fig. 2 in Dafni & Erez, 1987b).

4.5 *Why bother with deformities*

Abnormalities are deviations from the normal balanced and perfectly tuned growth processes shown by more than 99.9% of a non-disturbed urchin's population. Studying them is justified if it provides insight into the normal developmental processes. The fact that the deformities are well described in mechanical terms, e.g. aboral collapse, or Amb constrictions (= pinches), and correlated to the activity of elastic and contractile elements, provides sufficient support to the aforementioned biomechanical model. The recent profusion of papers dealing with echinoid growth models (Dafni, 1983b; 1986; Dafni & Erez, 1982; Baron, 1991; Ellers & Telford, 1992; Ellers et al., 1998; Johnson et al., 2002; Gudo, 2005) is indirectly related to our records of mass-deformities, and the insight we gained from it. Furthermore, confirmations of our hypotheses on the factors that cause deformity are testimony to these models' relevance and validity.

5 ACKNOWLEDGEMENTS

I thank my friend Prof. J. Erez for letting me experiment in his laboratory, and advised and encouraged me throughout these studies, and the staff of H. Steinitz Marine Laboratory in Eilat. I am also indebted to Prof. T.A. Ebert, who read an earlier version of this paper, and his comments are highly appreciated.

Readers who might have or obtain any information on similar mass deformities, in *Tripneustes* or any other sea urchin please contact me by Email: jdafni@gmail.com.

6 REFERENCES

Allain, J.Y. 1978. Déformations du test chez l'oursin *Lytechinus variegatus* (Lamarck) de la baie de Carthagene. *Caldasia* 12: 363-375.

Baron, C.J., 1991, The structural mechanics and morphogenesis of extant regular echinoids having rigid tests. Ph.D. Dissertation, University of California, Berkeley. 269 pp.

Dafni, J. 1980. Abnormal growth patterns in the sea urchin *Tripneustes cf. gratilla* (L.) under pollution (Echinodermata: Echinoidea). *J. exp. mar. Biol. Ecol.* 47: 259-279.

Dafni, J. 1983a. A new subspecies of *Tripneustes gratilla* (L.) from the northern Red Sea (Echinodermata: Echinoidea: Toxopneustidae). *Isr. J. Zool.* 32: 1-12.

Dafni, J. 1983b. Aboral depressions in the tests of the sea urchin *Tripneustes cf. gratilla* (L.) in the Gulf of Eilat, Red Sea. *J. exp. mar. Biol. Ecol.* 67: 1-15.

Dafni, J. 1986. A biomechanical model for the morphogenesis of regular echinoid tests. *Paleobiology*. 12: 143-160.

Dafni, J. 1992. Growth rate of the sea urchin (*Tripneustes gratilla elatensis*). *Isr. J. Zool.* 38: 25-33.

Dafni, J. & Erez, J., 1982. Differential growth in Tripneustes gratilla (Echinoidea). In: Lawrence, J. M. (ed.) *Intern Echinoderm Conf., Tampa Bay*: 71-75. Rotterdam: Balkema.

Dafni, J. & Erez, J., 1987a. Skeletal calcification patterns in the sea urchin *Tripneustes gratilla elatensis* (Echinoidea: Regularia) I. Basic patterns. *Mar. Biol.* 95: 275- 287.

Dafni, J. & Erez, J., 1987b. Skeletal calcification patterns in the sea urchin *Tripneustes gratilla elatensis* (Echinoidea: Regularia) II. Effect of various treatments. *Mar. Biol.* 95: 289-297.

Ebert, T.A. 1975. Growth and mortality of post-larval echinoids. *Amer. Zool*. 15:755-775.

Ebert. T.A. 1982. Longevity, life history, and relative body wall size in sea urchins. *Ecol. Monogr.* 52: 353-394.

Ebert, T.A. 1988. Allometry, design and constraint of body components and of shape in sea urchins. *J. Nat. Hist.*, 22: 1407-1425.

Ellers, O. 1993. A mechanical model of growth in regular sea urchins: predictions of shape and a developmental morphospace. *Proc. R. Soc. Lond.* B 254: 123-129.

Ellers, O. & Telford, M. 1992. Causes and Consequences of Fluctuating Coelomic Pressure on Sea Urchins. *Biol. Bull.* 182: 424-434

Ellers, O., Johnson, A.S. & Morberg, P. 1998. Sutural strengthening of urchin skeletons by collagenous sutural ligaments. *Biol. Bull.* 195: 136-144.

Gudo, M. 2005. An Evolutionary Scenario For The Origin Of Pentaradial Echinoderms—Implications From The Hydraulic Principles Of Form Determination. *Acta Biotheoretica* 53: 191-216

Harkness, R.D. 1968. Mechanical properties of collagenous tissues. Vol. 2A, pp. 247-310; in B.S. Gould (ed.), *Treatise on Collagen*. New York: Academic Press.

Johnson, A.S., Ellers, O., Lemire, J. Minor, M. & Leddy, H.A., 2002. Sutural loosening and skeletal flexibility during growth: Determination of drop-like shapes in sea urchins. *Proc. R. Soc. Lond.* B. 269: 215-220

Märkel, K. 1975. Wachstum des Coronarskeletes von *Paracentrotus lividus* Lmk. (Echinodermata, Echinoidea) *Zoomorphologie* 82: 259-280.

Moore, H.B. 1974. Irregularities in the test of regular sea urchins. *Bulletin of Marine Science* 24: 545-560.

Mortensen, T. 1943. *A Monograph of the Echinoidea.* Vol. 3(2), C.A. Reitzel, Copenhagen. 533 pp.

Moss, M.L. & Meehan, M. 1967. Sutural connective tissue in the test of an echinoid, *Arbacia punctulata. Acta Anatomica* 66: 279-304.

Seilacher, A. 1979. Constructional morphology of sand dollars. *Paleobiology* 5: 191-221

Trotter, J.A & Koob, T.J. 1995. Evidence that calcium-dependent cellular processes are involved in the stiffening response of holothurian dermis and that dermal cells contain an organic stiffening factor. J. Exp. Biol. 198: 1951-1961.

Wilkie, I.C. 1996. Mutable collagenous tissues: extracellular matrix as mechano-effector. Pp. 61-102 in *Echinoderm Studies* 5, M. Jangoux and J.M. Lawrence, eds. Balkema, Rotterdam.